ADVANCED MATERIALS

DOI: 10.1002/adma.200602886

A Novel Thermosetting Gel Electrolyte for Stable Quasi-Solid-State Dye-Sensitized Solar Cells**

By *Jihuai Wu*,* *Zhang Lan*, *Jianming Lin*, *Miaoliang Huang*, *Sancun Hao*, *Tsugio Sato*, and *Shu Yin*

Since the prototype of a dye-sensitized solar cell (DSSC) was reported in 1991 by O'Regan and Grätzel,[1] it has aroused intensive interest over the past decade due to its low cost and simple preparation procedure.[1,2] Based on liquid electrolytes, a photoelectric conversion efficiency of 11 % for DSSC has been achieved.[3,4] However, the potential problems caused by the liquid electrolytes, such as the leakage and volatilization of liquid, is considered as some of the critical factors limiting the long-term performance and practical use of the DSSCs. Thus, solid-state and quasi-solid-state electrolytes, such as polymer gel electrolytes, organic hole conductors and inorganic p-type semiconductors, [5–17] were attempted to replace the liquid electrolytes. However, due to low ionic conductivity, imperfect soakage of porous TiO_2 film and poor contact with counter electrode, the photoelectric conversion efficiency of DSSCs based on the solid-state electrolytes were less than 5 %. If an electrolyte can avoid the leakage and volatilization of liquid electrolyte and keep a high ionic conductivity and good interface contact with porous TiO_2 film and counter electrode, it is possible to accelerate the practical application of DSSCs. Gel electrolyte is one kind of electrolyte according with the above prerequisites, especially these thermo-irreversible (Thermosetting) gel electrolytes, which show high ionic conductivity, perfect interface contact, excellent chemical stability and temperature tolerance.[6,8,18–21]

Here, we report a novel thermosetting gel electrolyte (TSGE) based on poly (acrylic acid)-(ethylene glycol) (PAA-PEG) hybrid absorbing liquid electrolyte. It is known that poly (acrylic acid) (PAA) is a superabsorbent with 3D networks structure and hydrophilic groups, it can absorb large amount of liquid and the absorbed liquid is hard to be released even under some pressure.[22,23] However, pure PAA is not a good absorbent for conventional organic solvents used in liquid electrolytes. By modifying with amphiphilic poly (ethylene glycol) (PEG), the PAA-PEG hybrid shows a high absorbent ability for liquid electrolytes and the absorbed liquid electrolytes are hard to be leaked and volatilized for a long time. On the other hand, due to large amount of liquid is contained in the PAA-PEG hybrid, the ionic conductivity and interface soakage ability of the PAA-PEG hybrid is superior to that of solid-state electrolyte or other polymer gel electrolyte. The absorbed liquid electrolyte is kept in the networks of the hybrid due to hydrogen bonding between carboxylic groups and ether groups in the hybrid. Moreover, through reaction between Lewis basic organic solvents and the polyacid hybrid (PAA-PAG), a part of solvents is hanging on the polymer chains. Consequently, an electrolyte with thermosetting character and good stability, and with advantages for both liquid electrolyte and solid state electrolyte can be expected. Based on the TSGE, the DSSC shows a high photoelectric conversion efficiency and stability.

The dry pure PAA is a kind of rigid material and is hard for organic solvent to penetrate into. By modifying it with amphiphilic PEG, the hybrid became soft and could swell in organic solvents. The microstructure of the swollen TSGE is microporous. It is affected by the different molecular weight of PEG in modifying PAA as shown in Figure 1. Microporous pores can not be seen in the sample of PAA-PEG 400 while they

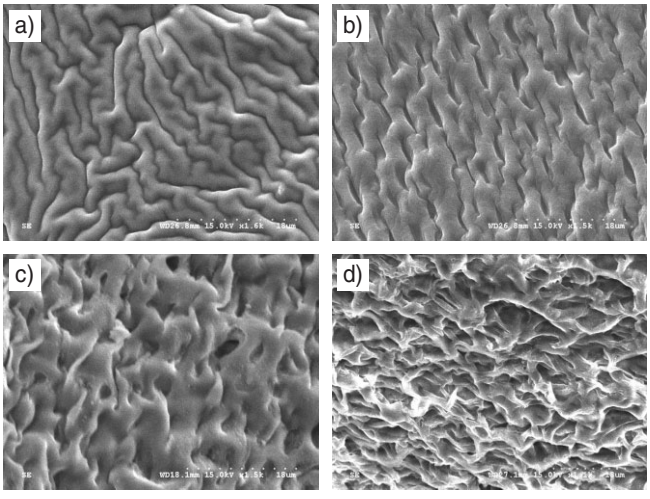

Figure 1. Scanning electron micrograph of cross-sectional view of the configuration of the swollen hybrids in optimized liquid electrolyte. a) PAA-PEG 400, b) PAA-PEG 1000, c) PAA-PEG 6000, d) PAA-PEG 20000; The composition of optimized liquid electrolyte is 0.5 M NaI, 0.05 M I_2, 0.4 M pyridine in 30 vol % NMP and 70 vol % GBL mixed solvents.

[*] Prof. J. H. Wu, Dr. Z. Lan, Prof. J. M. Lin, Prof. M. L. Huang, Dr. S. C. Hao
Institute of Materials Physical Chemistry, Huaqiao University
Quanzhou, 362021 (P.R. China)
E-mail: jhwu@huq.edu.cn
Prof. T. Sato, Dr. S. Yin
Institute of Multidisciplinary Research for Advanced Materials (IMRAM), Tohoku University
1-1 Katahira 2-Chome, Aoba-ku, Sendai 980-8577 (Japan)

[**] This work was supported by a grant from the National Natural Science Foundation of China (No. 50572030, No. 50372022) and the Functional Nanomaterials Scientific Special Program of Fujian Province, China (No. 2005HZ01-4).

can be observed in the other samples and the size of microporous pores increases with increasing PEG molecular weight in the hybrids. This microstructure of TSGE makes for well swelling ability of the hybrid in liquid electrolyte and excellent stability of the swollen hybrid by trapping absorbed liquid electrolyte in microporous.

The existence of hydrogen bonding between the hydroxyl and carboxylic groups on PAA and the ether oxygen groups or hydroxyl groups on PEG is another important factor for the excellent stability of TSGE.[24] It can be proved by the ATR-FTIR spectroscopy. The sample of PAA-PEG 1000 was selected to measure and a pure PAA was also measured for comparison. As shown in Figure 2, in pure PAA spectra (a), the bands at 3510 cm^{-1} and 3190 cm^{-1} are related to the free

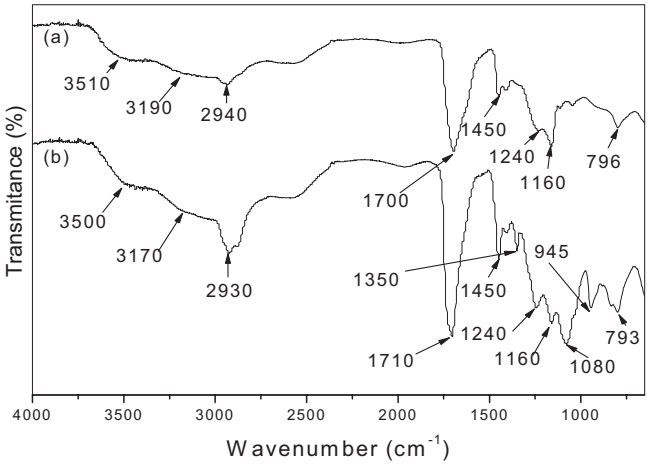

Figure 2. ATR-FTIR spectra of PAA (a) and PAA-oligo-PEG hybrid with equivalent mole ratio of carboxylic/ether groups (b).

hydroxyl groups and the hydroxyls forming hydrogen bonds, respectively.[25,26] These bands shift to a lower wavenumbers in the hybrid spectra (b) which is caused by changes in hydrogen bonding from self-associated hydrogen bonds on PAA to hydrogen bonds between carboxylic acid groups and ether oxygen groups on polymer chains.[27] The maximum of carbonyl band in pure PAA spectra lies at 1700 cm^{-1}, while in the hybrid, the band shifts to higher wavenumber (from 1700 cm^{-1} to 1710 cm^{-1}). Thus, it can be concluded that some self-associated hydrogen bonds in PAA are replaced by new inter-associated hydrogen bonds between polymer chains on PAA and oligo-PEG. The wavenumber in 1400–800 range is identified as ether bond in the chains of oligo-PEG. The bands at 1350 cm^{-1} and 945 cm^{-1} are associated with wagging motion and stretching vibration of CH_2 groups, respectively. The band at 1080 cm^{-1} is corresponding to stretching vibration of ether groups. All these bands in the hybrid spectra show that the chains of PAA and oligo-PEG bound together with the hydrogen bonds.

The adsorption mechanism of the PAA-PFG hybrid in organic solvent is based on the mild crosslinking 3D structure and hydrophilic groups on the PAA-PAG hybrid, as well as the interaction between the Lewis basic liquid electrolyte and polyacid character of the hybrid. For this reason, we adopted 0.5 M NaI and 0.05 M I_2 as electrolyte, which has been proven successful in our previous work.[24] γ-butyrolactone (GBL) and *N*-methyl pyrrolidone (NMP) both with high donor number were selected as mixed organic solvents. According to the definition of Lewis acid and Lewis basic, the higher donor number of organic solvent shows higher Lewis basicity. By controlling the volume ratio of two organic solvents, the optimized Lewis basic mixed organic solvents can be obtained. Moreover, the organic solvents of GBL and NMP both have high dielectric constants and low viscosity which are good solvent for inorganic iodide and obtaining high ionic conductivity. Further, they both have low melting point, high boiling point and low volatility which are propitious to obtaining high stable TSGE. Table 1 shows the physical characteristics of GBL and NMP.

Table 1. Data of physical characteristics of organic solvents.

Solvent	T_{mp} [°C]	T_{bp} [°C]	ε_r	Viscosity [cP]	DN	δ [$mScm^{-1}$] [a]
GBL	–44	204	42.0	1.70	18.0	9.60
NMP	–24.4	203	32.2	1.65	27.3	7.76

[a] Electrolyte contains 0.5 M NaI, 0.05 M I_2.

Figure 3 shows liquid electrolyte absorbency and ionic conductivity of TSGE in liquid electrolyte with different volume ratio of NMP in organic mixed solvents. With increasing volume ratio of NMP in mixed solvents, the Lewis basicity of mixed solvents increases, which causes the breakage of hydrogen bonds and easy penetration of liquid electrolyte into the hybrid, so the liquid electrolyte absorbency has a huge increase. When further increasing volume ratio of NMP in mixed

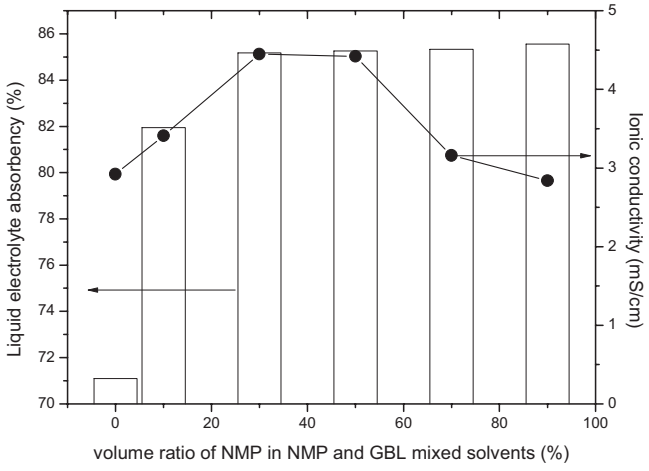

Figure 3. Liquid electrolyte absorbency and ionic conductivity of TSGE as functions of volume ratio of NMP in NMP + GBL mixed solvents.

ADVANCED MATERIALS

solvents, the reaction between Lewis basic liquid electrolyte and polyacid hybrid becomes equilibrium. The effect of increasing Lewis basicity on the enhancing liquid electrolyte absorbency is not obvious. It can be seen from Figure 3, the ionic conductivity of TSGE is affected by the liquid electrolyte absorbency. For liquid electrolyte (without PAA-PEG), with increasing volume ratio of NMP in mixed solvents, the ionic conductivity decreases, due to decrease of dielectric constants of mixed solvents. However, for TSGE, the ionic conductivity firstly increases and then decreases. This is due to the change of ions transport environment in TSGE. The first increase of ionic conductivity of TSGE is caused by the increase of liquid electrolyte absorbency. It leads to the formation of sufficiently swollen hybrid network and continuous organic solvent phase in TSGE, which decrease the resistance of PAA-PEG hybrid matrix on ions transport. The formation of continuous organic solvent channel in TSGE with the increase of liquid electrolyte absorbency also makes for ions transport. On the other hand, the conductivity depends on the dielectric constant of the mixture solvent. The decrease of dielectric constants of mixed solvents with increased volume ratio of NMP in liquid electrolyte mainly answers for the later decrease of ionic conductivity of TSGE. The optimized components of mixed organic solvents are 30 vol % NMP and 70 vol % GBL. Meanwhile, the components of organic mixed solvent makes for the best performance of DSSCs using liquid electrolyte.[26]

Besides the influence of components of mixed organic solvents on liquid electrolyte absorbency and ionic conductivity, the molecular weight of PEG and the mol ratio of PEG used in the hybrid also play an important role in the liquid electrolyte absorbency and ionic conductivity of TSGE. Figure 4 shows the influences of the molecular weight of PEG and the mole ratio of PEG 20000 used in the hybrids on the liquid electrolyte absorbency and ionic conductivity of TSGE. The hybrid with high molecular weight of PEG has high liquid electrolyte absorbency. Due to amphiphilic character of PEG, the hybrid contains higher mole ratio of PEG shows easier swelling in organic liquid electrolyte. It can be seen obviously that higher liquid electrolyte absorbency causes higher ionic conductivity. This is due to the same reason as aforementioned. Therefore, through controlling above factors, the highest ionic conductivity of TSGE about 6.12 $mS \cdot cm^{-1}$ can be obtained. This value is very close to liquid electrolyte (9.13 $mS \cdot cm^{-1}$) containing the same components. Quasi-solid-state DSSCs using the optimized TSGE will show high photovoltaic performance and stability.

The influence of donor numbers and electric additives on the ionic conductivity and interface contact quality of TSGE also was investigated. It was found that 30 vol % NMP and 70 vol % GBL was an optimized components for improving the donor numbers.[26] This component is the same as optimized mixed organic solvents for high liquid electrolyte absorbency of TSGE. The electric additive of pyridine has the similar function as 4-*tert*-butylpyridine for improving interface soakage, restraining dark current, and enhancing photovoltaic performance of DSSCs.[28]

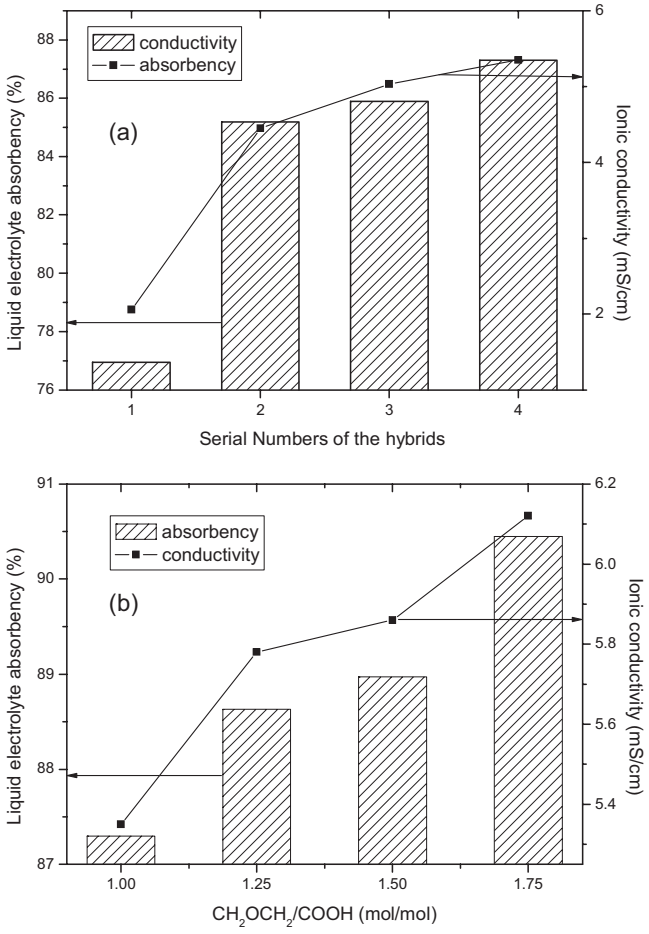

Figure 4. Liquid electrolyte absorbency and ionic conductivity of TSGE as functions of molecular weight of PEG used in the hybrid (a) and mol ratio of ether/carboxylic groups in the hybrid (b). (The serial numbers represent the samples the same as Fig. 1, the mol ratio of ether/carboxylic groups of (a) is 1/1; the molecular weight of PEG is 20000, the sample prepared by adding 0.1 wt % weight of acrylic acid monomers cross linker: *N*,*N*′-methylene bisacrylamide).

The photocurrent density versus voltage curves of DSSCs using different electrolytes are presented in Figure 5. The parameters of photovoltaic performance are listed in Table 2. The photovoltaic performance of DSSCs using liquid electro-

Table 2. The photovoltaic performance of DSSCs with different electrolytes.

Electrolyte	σ [$mS \cdot cm^{-1}$]	V_{OC} [V]	J_{SC} [$mA \cdot cm^{-2}$]	FF	η [%]
Liquid **a** [a]	9.13	0.632	14.78	0.613	5.73
Liquid **b** [b]	8.64	0.705	13.34	0.712	6.70
TSGE [c]	6.12	0.735	12.55	0.661	6.10

[a] Liquid **a**: containing 0.5 M NaI, 0.05 M I_2 in 30 vol. % NMP and 70 vol. % GBL mixed solvents.
[b] Liquid **b**: adding 0.4 M PY into Liquid **a**.
[c] TSGE: thermosetting gel electrolyte prepared by soaking the hybrid in liquid **b**.

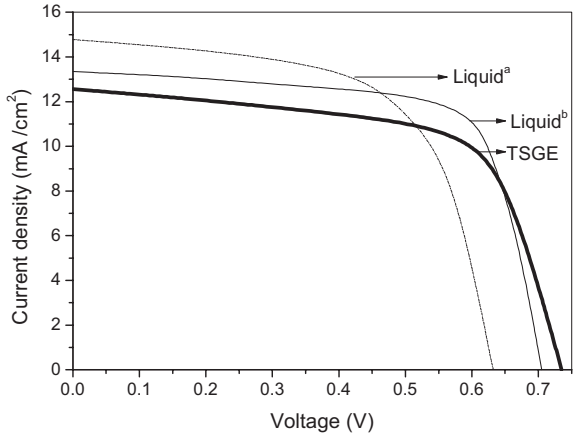

Figure 5. Photocurrent–photovoltage curves of DSSCs using different electrolytes. The parameters are listed in Table 2.

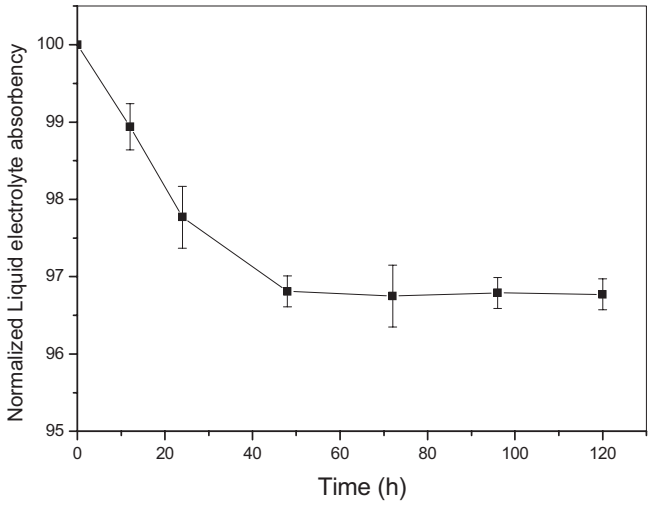

Figure 6. Normalized liquid electrolyte absorbency as functions of storage time at 30 °C [CH_2OCH_2 (mol)/COOH (mol) = 1.75/1, TSGE contains liquid **b**].

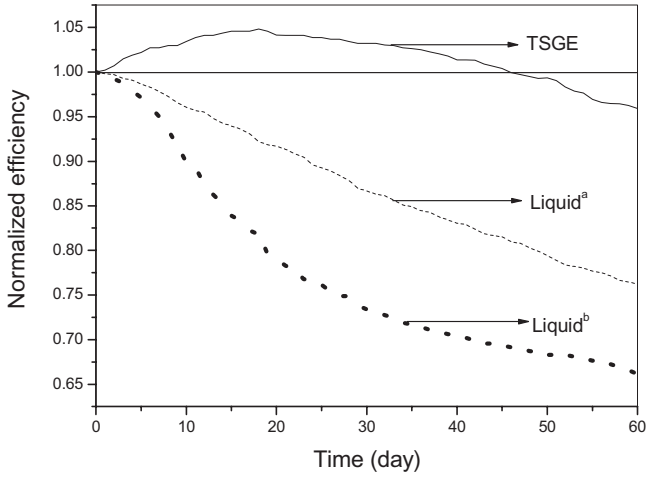

Figure 7. Time-course changes of the normalized efficiency of the DSSCs with liquid **a**, liquid **b** and TSGE.

lyte is well optimized by adding 0.4 M pyridine into electrolyte. The quasi-solid-state DSSC containing optimized TSGE shows high light-to-electricity conversion efficiency of 6.10 %. The value is 91 % of DSSC containing the optimized liquid electrolyte. The quasi-solid-state DSSC shows little lower short-circuit current density and higher open-circuit voltage than that of liquid electrolyte. Due to the soft and elastic state of the TSGE, it can form very thin electrolyte layer between two electrodes in cell. The high liquid electrolyte absorbency causes a sufficient extended organic subphase in TSGE, which is good for obtaining perfect interface contact between electrolyte layer and dye-coated TiO_2 film and counter electrode. The above reasons together with high ionic conductivity of TSGE lead to high photovoltaic performance of quasi-solid-state DSSC.

Due to the 3D structure of TSGE, the absorbed liquid electrolyte is kept in the microporous pores and the networks formed by hydrogen bonds between carboxylic groups and ether groups in the hybrid. Moreover, through reaction between Lewis basic organic solvents and polyacid hybrid, a part of solvents is hanging on the polymer chains. So the TSGE shows excellent stability as shown in Figure 6. It is the source of excellent long-term stability of DSSCs using TSGE. The data of DSSCs using liquid electrolytes were also measured for comparison as shown in Figure 7. All the samples were sealed as the procedures expressed in the Experimental. The samples were stored in a desiccator at ambient condition and measured once per day at room temperature under AM 1.5 irradiation. The values of light-to-electricity conversion efficiency were normalized to that of fresh ones. During the first eighteen days, the light-to-electricity conversion efficiency of quasi-solid-state DSSCs using TSGE increased slightly. This is due to the penetration of electrolyte through the nanoporous dye-coated TiO_2 electrode. The two electrodes are clipped by clinchers, so there are some pressures on the electrolyte layer in quasi-solid-state DSSCs. Under these pressures, the electrolyte can be pressed into nanoporous dye-coated TiO_2 electrode. On the other hand, the hybrid contains PEG-20000. It has small radius of gyration and can easily penetrate into the nanoporous dye-coated TiO_2 electrode.[29] The interfacial contact is improved by storing cells for some days. So the performance of cells becomes better. It maintained 95 % of original value of light-to-electricity conversion efficiency. This result is very significant for this kind of cell without rigorous sealing procedures. However, the things for DSSCs using liquid electrolytes under the same condition are not optimistic. The light-to-electricity conversion efficiency of DSSCs using liquid electrolyte **a** and **b** decreases during the measuring time. For DSSCs using liquid electrolyte **b**, firstly, the efficiency decreased quickly and then slowly. This is due to the volatilisation of pyridine in liquid electrolyte. The pyridine is easier to volatilize than GBL and NMP. Due to its strong influence on

ADVANCED MATERIALS

photovoltaic performance, the volatilisation of pyridine causes quick decrease of efficiency. The things are different for quasi-solid-state DSSCs using TSGE. As aforementioned, pyridine is Lewis basic solvent, these mixed solvents are kept in networks of TSGE or hanging on the polymer chains, so they are stable. Therefore, this kind of TSGE shows a feasible way to manufacture dye-sensitized solar cells for practical uses.

In conclusion, a novel thermosetting gel electrolyte (TSGE) based on PAA-PEG hybrid was developed. The hybrid shows the unique character of superabsorbent (PAA), namely, it can absorb large amount of liquid electrolyte and the absorbed liquid is hard to be volatilized and leaked, TSGE possesses advantages of solid state electrolyte with long-term stability. On the other hand, due to the absorption of large amount of liquid electrolyte in TSGE, it also maintains the merits of liquid electrolyte used in DSSC such as high ionic conductivity, good soakage property with counter electrode and porous TiO_2 film. The preparation conditions were optimized as: 0.5 M NaI + 0.05 M I_2 as electrolyte; 30 vol % NMP +70 vol % GBL + 0.4 M PY as mixed solvents, polymer host PAA-PEG hybrid was synthesized by two-steps aqueous polymerization with AA and PEG 20000 crooslinking with *N*,*N*′-methylene bisacrylamide. By soaking the hybrid into the mixed organic liquid electrolyte, a novel thermosetting gel electrolyte with ionic conductivity of 6.12 mS cm^{-1} was obtained. Based on the TSGE, a DSSC with light-to-electricity conversion efficiency of 6.10 % was attained under AM 1.5 irradiation. The DSSC possessed a good long-term stability. These results make a feasible approach for DSSCs practical applications.

Experimental

PEG with average molecular weight of 400, 1000, 6000, 20000, acrylic acid monomers, ammonium persulfate, sodium pyrosulfite, titanium isopropoxide, nitric acid, glacial acetic acid, terpineol, ethyl cellulose, ethanol, γ-butyrolactone (GBL), *N*-methylpyrrolidone (NMP), pyridine (PY), *N*,*N*′-methylene bisacrylamide, sodium iodide and iodine were all A. R. grade and all purchased from Sinopharm Chemical Reagent Co., Ltd, China. All reagents were used without further treating.

Conducting glass plates (FTO glass, Fluorine doped tin oxide overlayer, sheet resistance 8 Ω·cm^{-2}, purchased from Hartford Glass Co. USA) were used as substrates for precipitating TiO_2 porous films. Sensitizing dye *cis*-[$(dcbH_2)_2Ru(SCN)_2$] and optical diffuser paste Ti-Nanoxide 300 were purchased from Solaronix SA.

PAA-PEG hybrids were synthesized by the following processes. Firstly, 4.4 g PEG with different molecular weight was dissolved in 5 ml deionized water under stirring, respectively. The mixture was marked as A. Secondly, oligo-PAA was prepared by prepolymerization in water solution. 7.2 ml acrylic acid monomers were dissolved in 5 ml deionized water under stirring. Sodium pyrosulfite with an equivalent mol ratio of ammonium persulfate (2 wt % of monomers) were used as room temperature redox initiators to initiate polymerization reaction, and the mixture was marked as B. When the mixture B became a viscous solution, the oligo-PAA was obtained. Thirdly, the mixture A was dropped into the mixture B slowly under vigorous stirring to form homogeneous hybrid at room temperature. The final hybrid was kept in the ambient environment for 1 h to turn the oligo-PAA to PAA because of the exothermic polymerization reaction. Finally, the hybrid was moved into a vacuum oven at 80 °C to remove the water in the hybrid. The samples for higher mole ratio than 1/1 were added 0.1 wt % weight of acrylic acid monomers of crosslinker *N*,*N*′-methylene bisacrylamide into mixture B before polymerization in order to obtain high stability of swollen samples. Thermosetting gel electrolyte was prepared by soaking the hybrid in liquid electrolyte. The latter was composed of 0.5 M NaI, 0.05 M I_2 in mixed organic solvents including GBL and NMP. Pyridine was used as electrolytic additive. Figure 8 shows the digital photograph of the hybrid before and after soaking in liquid electrolyte.

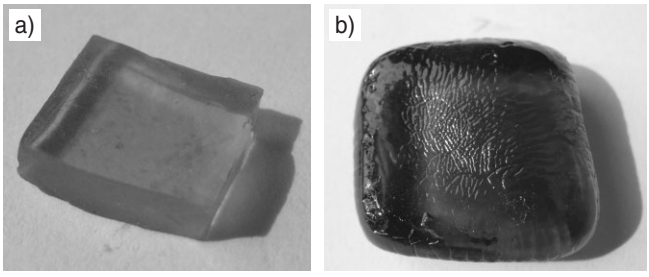

Figure 8. Digital photograph of the hybrid containing PEG 20000 (CH_2OCH_2 (mol)/COOH (mol) = 1) before (a) and after (b) soaking in liquid electrolyte.

The preparation of TiO_2 colloidal paste and double-layer film was according to the method reported by Wang.[30] The TiO_2 colloidal paste was used to fabricate the transparent film about 10 μm. Then the optical diffuser film about 4 μm was printed above the transparent film by using Ti-Nanoxide 300 paste. After sintering at 500 °C and cooling down to 80 °C, the double-layer nanostructured TiO_2 electrodes were dye-coated by immersing them into a 2.5×10^{-4} M absolute ethanol solution of *cis*-[$(dcbH_2)_2Ru(SCN)_2$] for 24 h.

$$Q_{le} = \frac{W - W_o}{W} \times 100\% \quad (1)$$

A quasi-solid-state dye-sensitized solar cell was fabricated by sandwiching a slice of thermosetting gel electrolyte between a dye-sensitized TiO_2 electrode and a platinum counter electrode. The two electrodes were clipped together and a cyanoacrylate adhesive was used as sealant. Epoxy resin was used for further sealing the cell.

ATR-FTIR measurements were carried out using a Nicolet Impact 410 FTIR spectrometer. The microcosmic structure of the swollen hybrid was measured using S-3500 N, HiTACHI. The liquid electrolyte absorbency (Q_{le}) of the hybrid was defined as:

$$FF = \frac{V_{max} \times J_{max}}{V_{oc} \times J_{sc}} \quad (2)$$

$$\eta(\%) = \frac{V_{max} \times J_{max}}{P_{in}} \times 100\% = \frac{V_{oc} \times J_{sc} \times FF}{P_{in}} \times 100\% \quad (3)$$

where W is the weight of swollen hybrid, and W_o is the original weight of dry hybrid. The Q_{le} values of samples were calculated according to Equation 1. Ionic conductivity was measured by using model DDB-6200 digitized conductivity meter (Shanghai Reici Instrument Factory, China). The instrument was calibrated with 0.01 M KCl aqueous solution prior to experiments.

The photovoltaic tests of quasi-solid-state dye-sensitized solar cells were carried out by measuring the *J–V* character curves under irradiation of white light from a 100 W xenon arc lamp (XQ-500W, Shanghai Photoelectricity Device Company, China) under ambient atmosphere. The incident light intensity and the active cell area were 100 $mW{\cdot}cm^{-2}$ and 0.2 cm^2 (0.4 × 0.5 cm^2), respectively. The fill factor (*FF*) and overall energy conversion efficiency (η) of the cell were calculated by the following equations:

where J_{SC} is the short-circuit current density ($mA{\cdot}cm^{-2}$), V_{OC} is the open-circuit voltage (V), Pin is the incident light power, and J_{max} ($mA{\cdot}cm^{-2}$) and V_{max} (V) are the current density and voltage in the *J–V* curves, respectively, at the point of maximum power output.

Received: December 18, 2006
Revised: July 3, 2007
Published online: October 31, 2007

[1] B. O'Regan, M. Grätzel, *Nature* **1991**, *353*, 737.
[2] M. Grätzel, *Nature* **2001**, *414*, 338.
[3] M. Grätzel, *Inorg. Chem.* **2005**, *44*, 6841.
[4] M. Grätzel, *J. Photochem. Photobiol. A* **2004**, *164*, 3.
[5] G. R. Kumara, S. Kaneko, M. Okuya, K. Tennakone, *Langmuir* **2002**, *18*, 10493.
[6] E. Stathatos, P. Lianos, A. S. Vuk, B. Orel, *Adv. Funct. Mater.* **2004**, *14*, 45.
[7] W. Kubo, T. Kitamura, K. Hanabusa, Y. Wada, S. Yanagida, *Chem. Commun.* **2002**, 374.
[8] E. Stathatos, P. Lianos, U. Lavrencic-Stangar, B. Orel, *Adv. Mater.* **2002**, *14*, 354.
[9] P. Wang, S. M. Zakeeruddin, J. E. Moser, M. K. Nazeeruddin, T. Sekiguchi, M. Grätzel, *Nat. Mater.* **2003**, *2*, 498.
[10] L. Wang, S. Fang, Y. Lin, X. Zhou, M. Li, *Chem. Commun.* **2005**, 5687.
[11] J. Kruger, R. Plass, M. Grätzel, H. J. Matthieu, *Appl. Phys. Lett.* **2002**, *81*, 367.
[12] W. Kubo, Y. Makimoto, T. Kitamura, Y. Wada, S. Yanagida, *Chem. Lett.* **2002**, 948
[13] S. Anandan, S. Pitchumani, B. Muthuraaman, P. Maruthamuthu, *Sol. Energy Mater. Sol. Cells* **2006**, *90*, 1715.
[14] T. Stergiopoulos, I. M. Arabatzis, G. Katsaros, P. Falaras, *Nano Lett.* **2002**, *2*, 1259.
[15] J. H. Kim, M. S. Kang, Y. J. Kim, J. Won, Y. S. Kang, *Solid State Ionics* **2005**, *176*, 579.
[16] J. H. Wu, Z. Lan, D. B. Wang, S. C. Hao, J. M. Lin, Y. F. Huang, S. Yin, T. Sato, *Electrochim. Acta* **2006**, *51*, 4243.
[17] J. H. Wu, Z. Lan, D. B. Wang, S. C. Hao, J. M. Lin, Y. L. Wei, S. Yin, T. Sato, *J. Photochem. Photobiol. A* **2006**, *181*, 333.
[18] E. Stathtos, P. Lianos, C. Krontiras, *J. Phys. Chem. B* **2001**, *105*, 3486.
[19] E. Stathtos, P. Lianos, *Chem. Mater.* **2003**, *15*, 1825.
[20] R. Komiya, L. Han, R. Yamanaka, *J. Photochem. Photobiol. A* **2004**, *164*, 123.
[21] S. Sakaguchi, H. Ueki, T. Kato, T. Kadoa, R. Shiratuchi, *J. Photochem. Photobiol. A* **2004**, *164*, 117.
[22] J. H. Wu, J. M. Lin, M. Zhou, *Macromol. Rapid Commun.* **2000**, *21*, 1032.
[23] J. M. Lin, J. H. Wu, Z. F. Yang, M. L. Pu, *Macromol. Rapid Commun.* **2001**, *22*, 422.
[24] Z. Lan, J. H. Wu, D. B. Wang, S. C. Hao, J. M. Lin, Y. F. Huang, *Sol. Energy* **2006**, *80*, 1483.
[25] F. Atsushi, K. Ryoichi, Y. Ryohsuke, I. Ashraful, L. Y. Han, *Sol. Energy Mater. Sol. Cells* **2006**, *90*, 649.
[26] M. K. Nazeeruddin, A. Kay, I. Rodicio, R. Humphry-Baker, E. Mueller, P. Liska, N. Vlachopoulos, M. Grätzel, *J. Am. Chem. Soc.* **1993**, *115*, 6382.
[27] K. Halina, S. Aleksandra, *J. Photochem. Photobiol. A* **2006**, *180*, 46.
[28] H. Kusama, M. Kurashige, H. Arakawa, *J. Photochem. Photobiol. A* **2005**, *169*, 169.
[29] M. S. Kang, J. H. Kim, J. Won, Y. S. Kang, *J. Photochem. Photobiol. A* **2006**, *183*, 15.
[30] P. Wang, S. M. Zakeeruddin, P. Comte, R. Charvet, R. H. Baker, M. Grätzel, *J. Phys. Chem. B* **2003**, *107*, 14336.

